Different behaviors of diffusing diffusivity dynamics based on three different definitions of fractional Brownian motion

Wei Wang [1], Qing Wei [2], Aleksei V. Chechkin [1,3,4,5] and Ralf Metzler [1,5,*]

[1]*Institute of Physics & Astronomy, University of Potsdam, 14476 Potsdam, Germany*

[2]*LSEC, ICMSEC, Academy of Mathematics and Systems Science, Chinese Academy of Sciences, Beijing 100190, China*

[3]*Faculty of Pure and Applied Mathematics, Hugo Steinhaus Center, Wrocław University of Science and Technology, 50-370 Wrocław, Poland*

[4]*German-Ukrainian Core of Excellence, Max Planck Institute of Microstructure Physics, Weinberg 2, 06120 Halle, Germany*

[5]*Asia Pacific Centre for Theoretical Physics, Pohang 37673, Republic of Korea*

(Received 13 April 2025; accepted 9 June 2025; published 7 July 2025)

The effects of "diffusing diffusivity" (DD), a stochastically time-varying diffusion coefficient, are explored within the frameworks of three different forms of fractional Brownian motion (FBM): (i) the Langevin equation driven by fractional Gaussian noise (LE-FBM), (ii) the Weyl integral representation introduced by Mandelbrot and van Ness (MN-FBM), and (iii) the Riemann-Liouville fractional integral representation (RL-FBM) introduced by Lévy. The statistical properties of the three FBM-generalized DD models are examined, including the mean-squared displacement (MSD), mean-squared increment (MSI), autocovariance function (ACVF) of increments, and the probability density function (PDF). Despite the long-believed equivalence of MN-FBM and LE-FBM, their corresponding FBM-DD models exhibit distinct behavior in terms of MSD and MSI. In the MN-FBM-DD model, the statistical characteristics directly reflect an effective diffusivity equal to its mean value. In contrast, in LE-FBM-DD, correlations in the random diffusivity give rise to an unexpected crossover behavior in both MSD and MSI. We also find that the MSI and ACVF are nonstationary in RL-FBM-DD but stationary in the other two DD models. All DD models display a crossover from a short-time non-Gaussian PDF to a long-time Gaussian PDF. Our findings offer guidance for experimentalists in selecting appropriate FBM-generalized models to describe viscoelastic yet non-Gaussian dynamics in bio- and soft-matter systems with heterogeneous environments.

DOI: 10.1103/w8gv-3fxt

I. INTRODUCTION

Since Robert Brown first observed the erratic motion of micron-sized granules ejected by pollen grains suspended in water [1], this phenomenon, now known as Brownian motion (BM), has been detected in numerous thermal systems and has significantly influenced conceptual advances in nonequilibrium statistical physics. A major breakthrough came with Albert Einstein's work [2], which provided a statistical interpretation of BM. Einstein proposed that the particle position increments are independent random variables following a specific distribution, leading to the prediction of the linear growth of the mean-squared displacement (MSD) over time and a Gaussian probability density function (PDF) for the displacement. Building on similar contributions by William Sutherland [3], Marian Smoluchowski [4], and Paul Langevin [5], the theory of Brownian motion was firmly established. Notably, with the experimental work of Jean Perrin, sophisticated experiments on Brownian motion allowed to pinpoint Avogadro's number and thus lay the foundation for the atomic theory of matter [6].

With the recent advances in modern measurement techniques, in particular, single particle tracking, anomalous diffusion with a power-law growth of the MSD [7]

$$\langle x^2(t)\rangle = 2D_H t^{2H}, \tag{1}$$

where D_H is the generalized diffusion coefficient of physical dimension $[D_H] = \text{length}^2/\text{time}^{2H}$ and H is Hurst or anomalous diffusion exponent, has been observed across a wide range of spatiotemporal scales in various physical areas. Inter alia, these include systems in cellular biology [8–11], soft matter [12–14], finance [15,16], ecology [17–20], astrophysics [21], geophysics [22,23], and quantum physics [24]. "Subdiffusion" features anomalous diffusion exponents in the range $0 < H < 1/2$, while "superdiffusion" is realized for $1/2 < H$. BM corresponds to the special case $H = 1/2$, and $H = 1$ describes ballistic transport [7,25–29].[1]

*Contact author: rmetzler@uni-potsdam.de

[1]The Hurst exponent is used here due to its historical connotation with FBM. In anomalous diffusion literature, another popular notation uses the anomalous diffusion exponent $\alpha = 2H$.

Two prominent processes have proven particularly effective for the modeling of anomalous diffusion across various systems. One is the continuous time random walk [30–33] with randomly distributed waiting times τ between two successive jumps. When the associated waiting time PDF $\psi(\tau)$ has the scale-free form $\psi(\tau) \simeq \tau^{-1-\alpha}$ with $0 < \alpha < 1$ [31–35], the resulting motion is subdiffusive with $H = \alpha/2$. The second common anomalous diffusion process is fractional Brownian motion (FBM), initially introduced by Kolmogorov [36] and later formalized using stochastic integrals by Mandelbrot and van Ness [37]. An alternative formulation for FBM is based on the stochastic Langevin equation $dx(t)/dt = \sqrt{2D_H}\xi_H(t)$, which is driven by fractional Gaussian noise with the stationary autocovariance function (ACVF) $\langle \xi_H(t)\xi_H(t+\tau)\rangle \sim H(2H-1)\tau^{2H-2}$ for $\tau > 0$ and $0 < H \leqslant 1$. The ACVF is negative ("antipersistent") for subdiffusion and positive ("persistent") for superdiffusion. FBM is widely used to model diffusion in viscoelastic media [38,39], animal movement patterns [20], serotonergic brain fiber density profiles [40,41], and roughness in financial data [42]. FBM was studied under confinement by hard walls as well as potentials of the generic form $V(x) \propto |x|^c$ ($c > 0$), observing distinct non-equilibrium shapes of the stationary PDF [43–45] as well as multimodal states and nonconfinement in shallow potential [46,47]. More recently, FBM based on the fractional integral of Riemann-Liouville type originally introduced by Lévy [37] with nonstationary increments has garnered significant attention [48–50] in systems with nonequilibrated initial condition, see also [51].

Diffusion in heterogeneous media displays numerous anomalous characteristics [52]. In environments with "annealed" disorder,[2] the particle's motion can be described by a purely time-dependent diffusion coefficient, i.e., its diffusivity fluctuates over time. Such an annealed heterogeneous dynamics leads to the phenomenon of Brownian yet non-Gaussian motion, which has been observed in various complex systems [53–59]. In these processes, while the MSD remains linear over time, the PDF deviates from the Gaussian form, often exhibiting a distinct exponential shape that eventually crosses over to a Gaussian distribution after a characteristic time (not all experiments have a sufficiently large window to observe such a crossover). The concept of diffusing diffusivity (DD), in which the diffusion coefficient of the tracer particle itself becomes a time-dependent random process, was first proposed by Chubinsky and Slater [60]. Chechkin *et al.* [61] introduced a minimal DD model, in which the diffusion coefficient evolves according to the square of an Ornstein-Uhlenbeck process. Non-equilibrium initial conditions and other forms of random diffusivity processes were considered in [62,63]. An alternative DD formulation was presented by Tyagi and Cherayil [64]. Concurrently, Jan and Sebastian [65,66] formalize the DD model using a path integral approach.

Viscoelastic and correlated superdiffusive yet non-Gaussian phenomena have recently been observed in biological systems [11,12,67–71], motivating the extension of the DD concept to correlated processes such as FBM. In our earlier work [72,73], we introduced a minimal FBM-generalized DD model formulated on the basis of the Langevin equation description of FBM, exploring various diffusivity protocols. In particular, unexpected crossovers in the MSD were observed beyond the correlation time. More recently, FBM based on Lévy's Riemann-Liouville formulation with a random diffusivity was analyzed in [48]—in this work, no crossover behavior in the MSD was found. Despite the similarities shared by different FBM formulations, the combination with DD-driven dynamics turns out to affect significant differences. In this paper, we investigate FBM-generalized models based on the three representations of FBM and analyze the impact of the random diffusivity on the statistical dynamics, as quantified by the MSD, MSI, ACVF, and the PDF.

The paper is organized as follows. In Sec. II, we introduce the physical observables usually evaluated from experimental data. These will then be employed to characterize the different DD models. In Sec. III, we present the three definitions of FBM in detail and generalize them to FBM-DD models. In Sec. IV, we present the numerical approach to generate trajectories of the FBM-DD processes. Then, we present the statistical characteristics of these three FBM-DD models in Sec. V, including MSD, MSI, ACVF, and PDF. We summarize and discuss our results in Sec. VI. We also present a table summarizing the main results for comparison of the statistical properties of the three FBM-generalized DD models.

II. PHYSICAL OBSERVABLES

To characterize the average diffusive behavior of tracer particles, the conventional measurable is the MSD. It is calculated by averaging over an ensemble of trajectories $x_i(t)$ at time t, relative to each particle's initial position $x_i(0)$,

$$\langle x^2(t)\rangle = \frac{1}{N}\sum_{i=1}^{N}(x_i(t) - x_i(0))^2, \tag{2}$$

where N denotes the total number of trajectories.

The MSI, qualifying the displacement-increments during the lag time Δ starting at the physical time t, is defined as the mean-squared of the increment in the form [77]

$$\left\langle x_\Delta^2(t)\right\rangle = \langle [x(t+\Delta) - x(t)]^2\rangle. \tag{3}$$

For processes with stationary increments, the MSI equals the MSD $\langle x^2(\Delta)\rangle$ [77]. The MSI is equivalent to the structure function originally introduced by Kolmogorov and Yaglom in their studies on locally homogeneous and isotropic turbulence [78–81].

The correlation of increments along an ensemble of time traces $x(t)$ can be probed in terms of the ACVF

$$C^\delta(t,\Delta) = \delta^{-2}\langle x^\delta(t+\Delta)x^\delta(t)\rangle, \tag{4}$$

with the increment $x^\delta(t) = x(t+\delta) - x(t)$. This ACVF is useful to analyze the nature of the anomalous diffusion in the unconfined space [7,26].

[2]Loosely, we distinguish "quenched" disorder, when the particle experiences the same diffusivity value each time it revisits the same site, from annealed disorder, when the value changes at each new visit [25,74–76].

III. FBM-GENERALIZED DD MODEL

A. Representations of FBM

In this section, we introduce the three alternative forms of FBM. They all encode the identical power-law scaling (1) of the MSD in their original formulation with constant parameters in unconfined space. We then proceed to generalize these FBM processes by incorporating the DD dynamics of their diffusivity, modeled as the square of an Ornstein-Uhlenbeck process.

1. Mandelbrot and van-Ness definition of FBM

The most widely used representation of FBM, introduced by Mandelbrot and van-Ness (MN-FBM) [37] and often referred to as "FBM I" in literature [82], is defined for the Hurst exponent $0 < H < 1$ in the form

$$x_{\rm MN}(t) = \sqrt{2D_H V_H}\left\{\int_0^t (t-s)^{H-1/2} dB(s) + \int_{-\infty}^0 [(t-s)^{H-1/2} - (-s)^{H-1/2}] dB(s)\right\}, \quad (5)$$

where $B(t)$ denotes a standard Brownian motion and V_H is a constant given by [37,83]

$$V_H = \left[(2H)^{-1} + \int_0^{+\infty} ((1+z)^{H-1/2} - z^{H-1/2})^2 dz\right]^{-1} = \frac{\Gamma(2H+1)\sin(\pi H)}{\Gamma(H+1/2)^2}. \quad (6)$$

2. Langevin equation formulation of FBM

An alternative formulation of MN-FBM, especially widely used in physics literature, is defined through the overdamped Langevin equation, a process we refer to as LE-FBM [37,84],

$$\frac{dx_{\rm LE}(t)}{dt} = \sqrt{2D_H}\xi_H(t), \quad (7)$$

for $0 < H \leqslant 1$. Here, the driving fractional Gaussian noise has zero mean and ACVF

$$\langle \xi_H^2 \rangle_\Delta = \langle \xi_H(t+\Delta)\xi_H(t)\rangle = \frac{1}{2\delta^2}(|\Delta+\delta|^{2H} + |\Delta-\delta|^{2H} - 2\Delta^{2H}). \quad (8)$$

MN-FBM and LE-FBM are equivalent in the sense that they exhibiting the same MSD and stationary MSI

$$\langle x^2(\Delta)\rangle_{\rm LE,MN} = \langle x_\Delta^2(t)\rangle_{\rm LE,MN} = 2D_H\Delta^{2H} \quad (9)$$

as well as the same stationary ACVF

$$C^\delta_{\rm LE,MN}(\Delta) = 2D_H\langle \xi_H^2\rangle_\Delta. \quad (10)$$

In particular, when $\Delta \gg \delta$, the ACVF has the power-law decay

$$C^\delta_{\rm LE,MN}(\Delta) \sim 2D_H H(2H-1)\Delta^{2H-2}. \quad (11)$$

3. Riemann-Liouville formulation of FBM

Recently, growing attention has been paid to an alternative definition of FBM introduced by Lévy [37,85], which is based on the Riemann-Liouville fractional integral (RL-FBM) and referred to as the "FBM II" [82]. It is expressed as

$$x(t) = \int_0^t \sqrt{4D_H H}(t-s)^{H-1/2} dB(s), \quad (12)$$

for $H > 0$.

RL-FBM shares the same MSD with MN-FBM and LE-FBM,

$$\langle x^2(\Delta)\rangle_{\rm RL} = 2D_H\Delta^{2H}. \quad (13)$$

However, the MSI of RL-FBM is nonstationary [77,86]

$$\langle x_\Delta^2(t)\rangle_{\rm RL} = 4D_H H\Delta^{2H}\left[I_H\left(\frac{t}{\Delta}\right) + \frac{1}{2H}\right], \quad (14)$$

where the integral $I_H(z)$ is given by

$$I_H(z) = \int_0^z [(1+s)^{H-1/2} - s^{H-1/2}]^2 ds. \quad (15)$$

At short times $t \ll \Delta$, the MSI (14) is approximately identical to the MSD,

$$\langle x^2(\Delta)\rangle_{\rm RL} \sim 2D_H\Delta^{2H}. \quad (16)$$

At long times, $t \gg \Delta$, the value of the integral (14) is given by

$$I_H\left(\frac{t}{\Delta}\right) + \frac{1}{2H} \approx \frac{1}{V_H}, \quad (17)$$

and the MSI becomes approximately stationary in this long-time limit,

$$\langle x_\Delta^2(t)\rangle_{\rm RL} \sim \frac{2D_H\Gamma(H+1/2)^2}{\Gamma(2H)\sin(\pi H)}\Delta^{2H}. \quad (18)$$

It is worthwhile noting that the MSI of RL-FBM exhibits the same long-time scaling behavior $\simeq\Delta^{2H}$ as the MSD but differs in its prefactor.

The ACVF of RL-FBM is also nonstationary with the exact expression [49,77]

$$C^\delta_{\rm RL}(t,\Delta) = 2D_H H(2H-1) \times \left\{\frac{3-2H}{2}\Delta^{2H-2}\int_0^{t/\Delta} q^{H-1/2}(1+q)^{H-5/2}dq + \delta^{-1}\Delta^{2H-1}\int_{t/\Delta}^{(t+\delta)/\Delta} q^{H-1/2}(1+q)^{H-3/2}dq\right\}. \quad (19)$$

In particular for $t = 0$ the ACVF reads [77]

$$C^\delta_{\rm RL}(t,\Delta) \sim \frac{4D_H H(2H-1)\delta^{H-1/2}}{2H+1}\Delta^{H-3/2} \quad (20)$$

in the limit $\Delta \gg \delta$, and for long times $t \to \infty$, it becomes stationary with

$$C^\delta_{\rm RL}(t,\Delta) \sim \frac{2D_H H(2H-1)\Gamma(H+1/2)^2}{\Gamma(2H)\sin(\pi H)}\Delta^{2H-2}. \quad (21)$$

For all three models discussed here, when $H = 1/2$, the processes reduce to standard BM. As indicated above, the three definitions are valid for different ranges of the Hurst exponent H. Namely, for MN-FBM, the Hurst exponent needs to

be given by $0 < H < 1$, ensuring a positive prefactor $V_H > 0$. For LE-FBM, the Hurst exponent satisfies $0 < H \leqslant 1$. In the case of RL-FBM, there are no strict constraints on $H > 0$. In this study, we specifically focus on the range $0 < H < 1$.

B. Diffusing diffusivity

The random diffusivity $D(t)$ in the following is assumed to follow the square of an Ornstein-Uhlenbeck process $Y(t)$ [61],

$$D(t) = Y^2(t), \tag{22a}$$

$$\frac{d}{dt}Y(t) = -\frac{Y}{\tau} + \sigma\eta(t), \tag{22b}$$

where $\eta(t)$ is a zero-mean white Gaussian noise with ACVF $\langle\eta(t)\eta(t')\rangle = \delta(t-t')$, $D(t)$, and $Y(t)$ have physical units $[D] = \text{length}^2/\text{time}^{2H}$ and $[Y] = \text{length}/\text{time}^H$. Moreover, τ is the correlation or characteristic time of the Ornstein-Uhlenbeck process, and σ is the noise intensity for $D(t)$ with units $[\sigma] = \text{length}/\text{time}^{H+1/2}$.

We assume equilibrium initial conditions for $Y(t)$, i.e., $Y(0)$ is taken randomly from the equilibrium distribution

$$f_{\text{eq}}(Y) = \frac{1}{\sqrt{\pi\sigma^2\tau}}\exp\left(-\frac{Y^2}{\sigma^2\tau}\right). \tag{23}$$

Thus, the process $Y(t)$ is stationary with the effective diffusivity [61]

$$\langle D\rangle = \langle Y^2\rangle = \frac{\sigma^2\tau}{2}. \tag{24}$$

The second significant characteristic of the process $D(t)$ is the correlation function of the square root of $D(t)$ given by [72]

$$\begin{aligned} K(\Delta) &= \langle\sqrt{D(t)D(t+\Delta)}\rangle \\ &= \frac{\sigma^2\tau}{\pi}\left[\sqrt{1-e^{-2\Delta/\tau}}\right. \\ &\quad \left. + e^{-\Delta/\tau}\arctan\left(\frac{e^{-\Delta/\tau}}{\sqrt{1-e^{-2\Delta/\tau}}}\right)\right]. \end{aligned} \tag{25}$$

When time is much shorter than the characteristic time, $\Delta \ll \tau$, the diffusivity does not vary much and thus we have

$$\langle D\rangle = \lim_{\Delta\to 0} K(\Delta) = \frac{\sigma^2\tau}{2}. \tag{26}$$

When time is much longer than the characteristic time $\Delta \gg \tau$, the correlations of the diffusivity decay exponentially. For this approximate independence, we then have

$$K_{\text{eff}} = \lim_{\Delta\to\infty} K(\Delta) = \langle|Y(t)|\rangle^2 = \frac{\sigma^2\tau}{\pi}. \tag{27}$$

1. Diffusing-diffusivity-generalized FBM

We are now ready to define the three DD-generalized FBM models via introducing the DD dynamics (22) based on the three FBM representations.

MN-FBM-DD. Combining the definition (5) of MN-FBM with the DD dynamics (22), we obtain the MN-FBM-DD model:

$$\begin{aligned} x_{\text{MN}}(t) &= \int_0^t \sqrt{2V_H D(s)}(t-s)^{H-1/2}dB(s) + \int_{-\infty}^0 \sqrt{2V_H D(s)} \\ &\quad \times [(t-s)^{H-1/2} - (-s)^{H-1/2}]dB(s). \end{aligned} \tag{28}$$

In this case, the dynamics of the DD $D(t)$ is assumed to be at equilibrium at all times t, including $t \leqslant 0$.

LE-FBM-DD. Adding the DD dynamics to the LE-FBM model (7) leads us to the LE-FBM-DD model

$$\frac{dx_{\text{LE}}(t)}{dt} = \sqrt{2D(t)}\xi_H(t). \tag{29}$$

RL-FBM-DD. Finally, from the definition (9) of RL-FBM together with the DD dynamics, we find the RL-FBM-DD process

$$x_{\text{RL}}(t) = \int_0^t \sqrt{4HD(s)}(t-s)^{H-1/2}dB(s). \tag{30}$$

IV. SIMULATIONS SETUP

The discrete-time diffusivity $D(t_n) = Y^2(t_n)$ at time $t_n = n \times \delta t$, where δt is the time step, can be generated from the discretized Ornstein-Uhlenbeck process (22b),

$$Y(t_n) - Y(t_{n-1}) = -\frac{1}{\tau}Y(t_{n-1})\delta t + \sigma\eta(t_{n-1})\delta t, \tag{31}$$

where $\eta(t_n) = \eta_n/\sqrt{\delta t}$ and η_n is a normally distributed random variable with zero mean and unit variance. In practice, the discretized form (31) serves as an approximate method to simulate the Ornstein-Uhlenbeck process (22b) for small time steps. For any time step, an exact formula exists, as detailed in [87,88], given by

$$Y(t_n) = Y(t_{n-1})e^{-\delta t/\tau} + \eta_n\left[\frac{\sigma^2\tau}{2}(1-e^{-2\delta t/\tau})\right]^{1/2}. \tag{32}$$

It can be shown that when $\delta t \ll \tau$, Eq. (32) reduces, to first order in δt, to the approximate update formula (31). It is important to highlight that our study focuses on systems characterized by a well-defined characteristic timescale, i.e., $\tau \gg \delta t$, implying that the first-order approximation in δt for simulating the Ornstein-Uhlenbeck process (22b) is sufficient to accurately reproduce the statistical properties of the diffusivity (22a) and ensures full consistency with our theoretical predictions.

LE-FBM-DD. For the LE-FBM-DD model, we discretize the Langevin equation (29) such that

$$x_{\text{LE}}(t_n) - x_{\text{LE}}(t_{n-1}) = \sqrt{2D(t_{n-1})}\xi_H(t_{n-1})\delta t, \tag{33}$$

where $\xi_H(t_n) = \xi_{H,n}/(\delta t)^{1-H}$ and $\xi_{H,n}$ is the discrete sequence of fractional Gaussian noise with zero mean and unit variance, which can be generated from standard approaches [89–91]. In this paper, we employ the Wood-Chan method [92] due to its rapid simulation times achieved by using the discrete Fourier transformation.

RL-FBM-DD. For the RL-FBM-DD model, a direct approach to discretize the stochastic integral may be adopted in

the form

$$x_{\mathrm{RL}}(t_n) = \sum_{i=0}^{n-1} \sqrt{4HD(t_i)}\eta(t_i)\delta t \times (t_n - t_i)^{H-1/2}. \quad (34)$$

Typically, this direct approach is not very accurate for unveiling the scaling of statistical quantities when $H < 1/2$ as the weight $w(t_n - t_i) = (t_n - t_i)^{H-1/2}$ becomes excessively large when $t_n - t_i$ is small.

Instead, we discretize the stochastic integral in the form

$$x_{\mathrm{RL}}(t_n) = \sum_{i=0}^{n-1} \int_{t_i}^{t_{i+1}} \sqrt{4HD(s)}(t_n - s)^{H-1/2}\eta(s)ds. \quad (35)$$

A simple approach can be applied when $D(s) \approx D(t_i)$ and $\eta(s) \approx \eta(t_i)$ within the short-time interval $[t_i, t_{i+1}]$. In this case, we get

$$\begin{aligned} x_{\mathrm{RL}}(t_n) &= \sum_{i=0}^{n-1} \sqrt{4HD(t_i)}\eta(t_i) \int_{t_i}^{t_{i+1}} (t_n - s)^{H-1/2} ds \\ &= \sum_{i=0}^{n-1} \sqrt{4HD(t_i)}\eta(t_i)\delta t \\ &\quad \times \frac{(t_n - t_i)^{H+1/2} - (t_n - t_{i+1})^{H+1/2}}{(H+1/2)\delta t}. \end{aligned} \quad (36)$$

This form ensures that the power-law weight does not have any singularity. Alternatively, the weight function

$$w(t_n - t_i) = \left[\frac{(t_n - t_i)^{2H} - (t_n - t_{i+1})^{2H}}{2H\delta t}\right]^{1/2} \quad (37)$$

can be applied [93] to improve the prediction of the variance scaling properties; in our simulations, we adopt this protocol.

MN-FBM-DD. In analogy to the RL-FBM-DD model, for the MN-FBM-DD model, the discrete strategy can be formulated as

$$\begin{aligned} x_{\mathrm{MN}}(t_n) &= \sum_{i=-n_a}^{n-1} \sqrt{2V_H D(t_i)}\eta(t_i)\delta t \times w(t_n - t_i) \\ &\quad - \sum_{j=-n_a}^{0} \sqrt{2V_H D(t_j)}\eta(t_j)\delta t \times w(-t_j). \end{aligned} \quad (38)$$

In practice, choosing $n_a = (T/\delta t)^{3/2}$ is sufficient [90,91].

V. STATISTICAL PROPERTIES OF THE DD-GENERALIZED FBM MODELS

A. MSD

LE-FBM-DD. The MSD of LE-FBM-DD model (29) was analyzed in [72], finding

$$\langle x^2(t)\rangle_{\mathrm{LE}} = 4\int_0^t (t-s)K(s)\langle \xi_H^2\rangle_s ds. \quad (39)$$

Here $K(s)$ and $\langle \xi_H^2\rangle_s$ are given by Eqs. (25) and (8). Expression (39) reveals an intriguing crossover behavior: at short times $t \ll \tau$, the MSD reads

$$\langle x^2(t)\rangle_{\mathrm{LE}} \sim 4K(0)\int_0^t (t-s)\langle \xi_H^2\rangle_s ds \sim 2\langle D\rangle t^{2H}. \quad (40)$$

However, at long times $t \gg \tau$, different behaviors are emerging. For superdiffusion ($H > 1/2$), the MSD the scaling is identical to the short-time scaling, but with a different prefactor,

$$\langle x^2(t)\rangle_{\mathrm{LE}} \sim 2K_{\mathrm{eff}} t^{2H}. \quad (41)$$

In contrast, for subdiffusion ($H < 1/2$), the MSD crosses over to normal diffusion

$$\langle x^2(t)\rangle_{\mathrm{LE}} \sim 2D_{\mathrm{eff}} t. \quad (42)$$

Here, the effective diffusion coefficient K_{eff} is given by Eq. (27), and D_{eff} corresponds to the form

$$D_{\mathrm{eff}} = 2\int_0^\infty K(s)\langle \xi_H^2\rangle_s ds. \quad (43)$$

Analytically determining the exact diffusion coefficient D_{eff} is not feasible, but it was proved that they possess a finite value for $H < 1/2$ [72].

MN-FBM-DD. The MSD of the MN-FBM-DD (28) can be expressed as

$$\begin{aligned} \langle x^2(t)\rangle_{\mathrm{MN}} &= 2V_H\langle D\rangle \left\{ \int_0^t (t-s)^{2H-1} ds \right. \\ &\quad \left. + \int_{-\infty}^0 [(t-s)^{H-1/2} - (-s)^{H-1/2}]^2 ds \right\}. \end{aligned} \quad (44)$$

The variable transform $z = -s/t$ in Eq. (44) then yields

$$\begin{aligned} \langle x^2(t)\rangle_{\mathrm{MN}} &= 2V_H\langle D\rangle t^{2H} \left\{ \int_0^1 (1-z)^{2H-1} dz \right. \\ &\quad \left. + \int_0^{+\infty} [(1+z)^{H-1/2} - z^{H-1/2}]^2 dz \right\} \\ &= 2\langle D\rangle t^{2H}. \end{aligned} \quad (45)$$

RL-FBM-DD. Similarly, we obtain the MSD of the RL-FBM-DD model (30),

$$\begin{aligned} \langle x^2(t)\rangle_{\mathrm{RL}} &= 4H\langle D\rangle \int_0^t (t-s)^{2H-1} ds \\ &= 2\langle D\rangle t^{2H}, \end{aligned} \quad (46)$$

which is identical to result (45) for MN-FBM-DD.

Although the classic FBM based on the three representations analyzed here has the same MSD, the DD-generalized FBM models exhibit significantly different behaviors: the MSDs of the MN-FBM-DD and RL-FBM-DD models continuously evolve with a power-law scaling of t^{2H} for all Hurst exponents, with an effective generalized diffusion coefficient equal to the mean diffusivity; in contrast, for the LE-FBM-DD model the MSD exhibits a crossover from the short-time scaling $\simeq t^{2H}$ to the long-time behavior $\simeq t$ for subdiffusion. The simulations of the MSD for all three models are presented in Fig. 1 and show excellent agreement with the theoretical results.

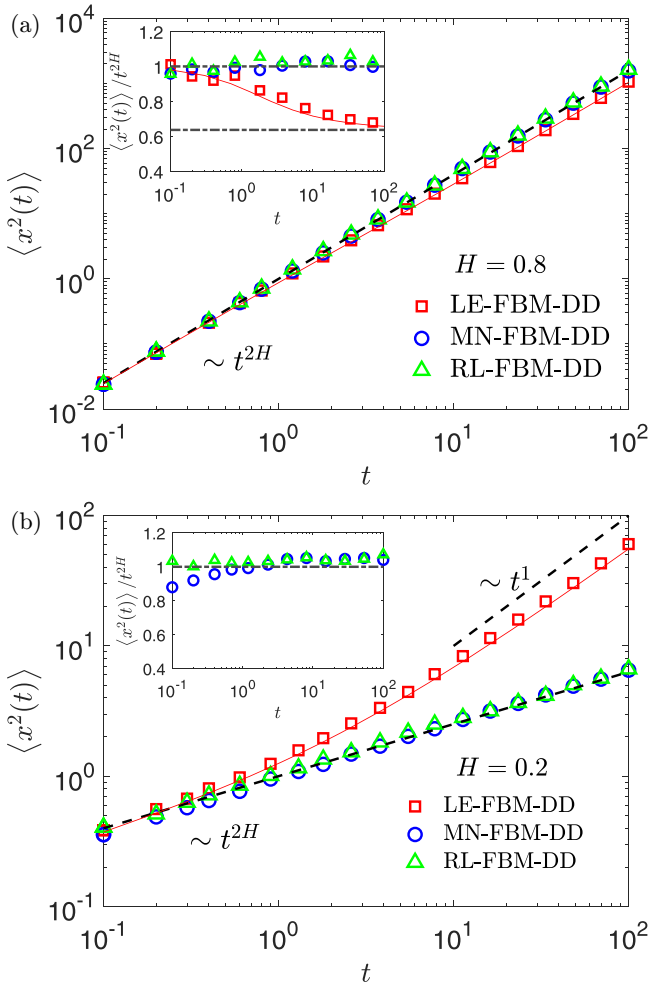

FIG. 1. Simulations (circles, triangles, and rectangles) for the MSD of the three DD-generalized FBM models with (a) $H = 0.8$ and (b) $H = 0.2$. The numerical evaluation of the MSD (39) of the LE-FBM-DD model (29) is depicted by the red solid curve. The generalized diffusion coefficients are displayed in the inset. In panel (a), the MSD of all models shows the same scaling, and the generalized diffusion coefficient $\langle x^2(t)\rangle/t^{2H}$ of the LE-FBM-DD has a crossover from $2\langle D\rangle = 1$ to $2K_{\rm eff} = 2/\pi$, represented by dash-dotted lines. In panel (b), the MSD of the LE-FBM-DD model switches from $2\langle D\rangle t^{2H}$ at short times to normal diffusion, $2D_{\rm eff}t$ at long times, while the MSD of the MN-FBM-DD and RL-FBM-DD models scale $\simeq t^{2H}$ at all times. Simulation parameters: $\tau = 1$, $\sigma = 1$, $dt = 0.1$, and $T = 100$. These parameters are consistently kept across all figures, unless stated otherwise.

B. MSI

LE-FBM-DD. The MSI of the LE-FBM-DD (29) model,

$$\left\langle x_\Delta^2(t)\right\rangle_{\rm LE} = 4\int_0^\Delta (\Delta - s)K(s)\left\langle \xi_H^2\right\rangle_s ds, \tag{47}$$

has the same expression as the MSD (39) and is stationary, i.e., solely depending on the lag time Δ. At short times, $\Delta \ll \tau$, the MSD behaves as

$$\left\langle x_\Delta^2(t)\right\rangle \sim 2\langle D\rangle\Delta^{2H}. \tag{48}$$

At long times we find

$$\left\langle x_\Delta^2(t)\right\rangle_{\rm LE} = \begin{cases} 2D_{\rm eff}\Delta, & H < 1/2 \\ 2K_{\rm eff}\Delta^{2H}, & H > 1/2 \end{cases}. \tag{49}$$

The effective diffusion coefficients $K_{\rm eff}$ for superdiffusive and $D_{\rm eff}$ for subdiffusive H are given by expressions (27) and (43), respectively.

MN-FBM-DD. The MSI of the MN-FBM-DD (28) model reads

$$\left\langle x_\Delta^2(t)\right\rangle_{\rm MN} = 2V_H\langle D\rangle\left\{\int_t^{t+\Delta}(t+\Delta-s)^{2H-1}ds + \int_{-\infty}^{t} \times[(t+\Delta-s)^{H-1/2} - (t-s)^{H-1/2}]^2 ds\right\}. \tag{50}$$

With the variable transform $z = s - t$, the same expression as (45) for the MSD of MN-FBM-DD can be obtained,

$$\left\langle x_\Delta^2(t)\right\rangle_{\rm MN} = 2V_H\langle D\rangle\left\{\int_0^\Delta(\Delta - z)^{2H-1}dz + \int_{-\infty}^{0}[(\Delta - z)^{H-1/2} - (-z)^{H-1/2}]^2 dz\right\}, \tag{51}$$

which leads to the stationary MSI

$$\left\langle x_\Delta^2(t)\right\rangle_{\rm MN} = 2\langle D\rangle\Delta^{2H}. \tag{52}$$

RL-FBM-DD. The MSI of RL-FBM (14) was analyzed in [77,86]. Here, we obtain the MSI of the RL-FBM-DD model in the form

$$\left\langle x_\Delta^2(t)\right\rangle_{\rm RL} = 4H\langle D\rangle\Delta^{2H}\left\{I_H\left(\frac{t}{\Delta}\right) + \frac{1}{2H}\right\}. \tag{53}$$

At short times $t \ll \Delta$, the MSI of RL-FBM-DD is identical to the MSD (46),

$$\left\langle x_\Delta^2(t)\right\rangle_{\rm RL} \sim 2\langle D\rangle\Delta^{2H}. \tag{54}$$

At long times $t \gg \Delta$, the MSI reads

$$\left\langle x_\Delta^2(t)\right\rangle_{\rm RL} \sim \frac{2\langle D\rangle\Gamma(H+1/2)^2}{\Gamma(2H)\sin(\pi H)}\Delta^{2H}. \tag{55}$$

From the MSIs of MN-FBM-DD and RL-FBM-DD, Eqs. (52) and (53), respectively, we find that the random diffusivity for MN-FBM-DD and RL-FBM-DD effects an effective diffusion coefficient. A crossover behavior similar to that observed in the MSD also appears in the MSI of the LE-FBM-DD model given by (47). We also note that the MSI is stationary in the LE-FBM-DD and MN-FBM-DD models but nonstationary in the RL-FBM-DD model. Figure 2 compares the results from simulations with the theoretical results for the MSI.

C. ACVF

LE-FBM-DD. The stationary ACVF of the LE-FBM-DD model (29) is given by

$$C_{\rm LE}^\delta(t,\Delta) = 2\langle\sqrt{D(t)}\sqrt{D(t+\Delta)}\rangle\langle\xi_H(t)\xi_H(t+\Delta)\rangle = 2K(\Delta)\left\langle\xi_H^2\right\rangle_\Delta. \tag{56}$$

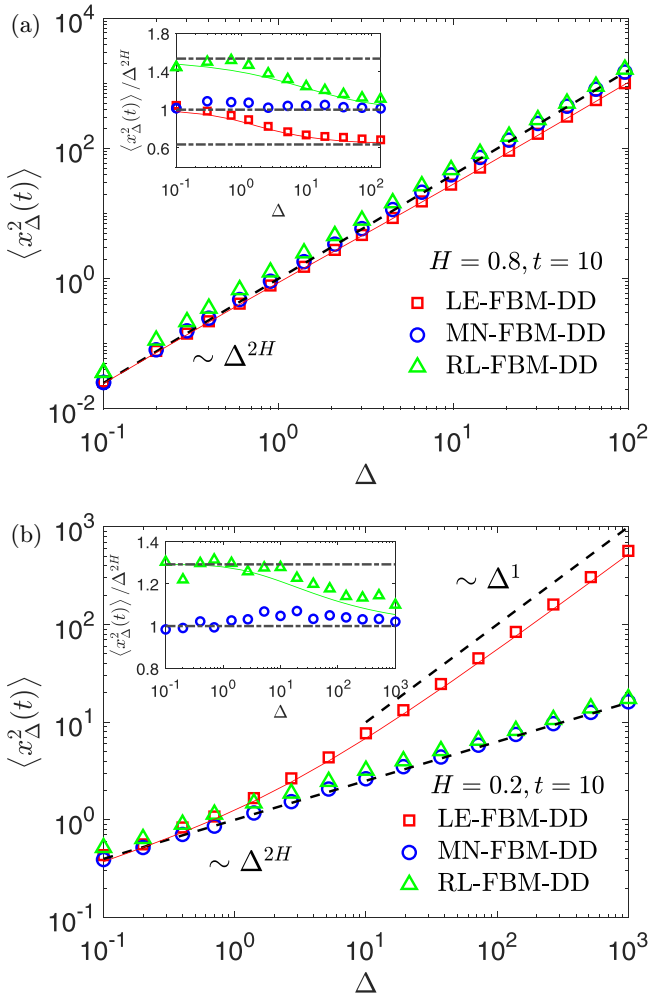

FIG. 2. Simulations (circles, triangles, and rectangles) for the MSIs with starting time $t = 10$ of the three DD-generalized FBM models with (a) $H = 0.8$ and (b) $H = 0.2$. The numerical evaluations of the MSIs (47) and (53) of LE-FBM-DD (29) and RL-FBM-DD (30) are represented by red and green curves, respectively. The generalized diffusion coefficients $\langle x^2(t)\rangle/t^{2H}$ are displayed in the inset. In panel (a) for the superdiffusive case, the MSIs of all models have the same scaling; the LE-FBM-DD-MSI has a crossover behavior in the prefactor of the MSI from $2\langle D\rangle = 1$ to $2K_{\rm eff} = 2/\pi$, while for RL-FBM-DD it crosses over from $\frac{2\langle D\rangle\Gamma(H+1/2)^2}{\Gamma(2H)\sin(\pi H)}$ to $2\langle D\rangle = 1$. In panel (b) for the subdiffusive case, the MSI of the LE-FBM-DD switches from $2\langle D\rangle\Delta^{2H}$ at short times to normal diffusion $2D_{\rm eff}\Delta$ at long times.

The correlation $K(\Delta)$ in Eq. (25) can be expanded at large lag times $\Delta \gg \tau$ up to second order, leading to

$$K(\Delta) \sim \sigma^2\tau(\pi^{-1} + e^{-2\Delta/\tau}), \tag{57}$$

from which the ACVF reads

$$C^\delta_{\rm LE}(\Delta) \sim 2\sigma^2\tau\left[\pi^{-1}\langle\xi^2_H\rangle_\Delta + e^{-2\Delta/\tau}\langle\xi^2_H\rangle_\Delta\right]. \tag{58}$$

This expression elucidates nicely the *a priori* unexpected crossover behavior in the MSD: The first part, proportional to the correlations of the fractional Gaussian noise, leads to anomalous diffusion characterized by the scaling $\simeq t^{2H}$ in the MSD at long times whereas the second part, governed by the truncated power-law noise correlation, contributes the normal-diffusive scaling $\simeq t^1$ at long times [84]. Especially, when $H < 1/2$, the linear MSD component dominates.

MN-FBM-DD. To obtain the ACVF of the MN-FBM-DD model (28), the correlation of the displacement must be considered, given by

$$\langle x_{\rm MN}(t+\Delta)x_{\rm MN}(t)\rangle = \langle D\rangle((t+\Delta)^{2H} + t^{2H} - \Delta^{2H}). \tag{59}$$

Substituting the correlation of the displacement into expression (4), one obtains the stationary ACVF

$$C^\delta_{\rm MN}(t,\Delta) = 2\langle D\rangle\langle\xi^2_H\rangle_\Delta. \tag{60}$$

In comparison with the ACVF of MN-FBM (10), the ACVF of the MN-FBM-DD model directly reflects an effective diffusion coefficient equal to the mean diffusivity.

RL-FBM-DD. Analogously, the ACVF of the RL-FBM-DD model (30) turns out to be equal to that of RL-FBM with an effective diffusion coefficient,

$$C^\delta_{\rm RL}(t,\Delta) = 2\langle D\rangle H(2H-1) \times\left\{\frac{3-2H}{2}\Delta^{2H-1}\int_0^{t/\Delta} q^{H-1/2}(1+q)^{H-5/2}dq + \delta^{-1}\Delta^{2H-1}\int_{t/\Delta}^{(t+\delta)/\Delta} q^{H-1/2}(1+q)^{H-3/2}dq\right\}. \tag{61}$$

Specifically, when $t = 0$, the approximate ACVF with $\Delta \gg \delta$ of RL-FBM-DD is

$$C^\delta_{\rm RL}(t,\Delta) \sim \frac{4\langle D\rangle H(2H-1)\delta^{H-1/2}}{2H+1}\Delta^{H-3/2}. \tag{62}$$

When $t \to \infty$, we find

$$C^\delta_{\rm RL}(t,\Delta) \sim \frac{2\langle D\rangle H(2H-1)\Gamma(H+1/2)^2}{\Gamma(2H)\sin(\pi H)}\Delta^{2H-2}. \tag{63}$$

To conclude this part, the correlations (25) of the random diffusivity emerges in the ACVF (56) of LE-FBM-DD, affecting the unexpected crossover behavior in the MSD and MSI. In contrast, the ACVF reflects the effective diffusion coefficient $\langle D\rangle$ for MN-FBM-DD and RL-FBM-DD, Eqs. (60), (62), and (63). Moreover, the ACVF is stationary for both LE-FBM-DD and MN-FBM-DD models, while it is nonstationary in the RL-FBM-DD model. The simulations for the ACVF are shown in Fig. 3.

D. PDF

Given that at short times $t \ll \tau$ the diffusivity following the Ornstein-Uhlenbeck dynamics changes little over time, single trajectories of all the three models behave as the corresponding FBM with constant diffusivity, and the PDFs can be described by a superstatistical approach [94], i.e., can be obtained as the average of a single Gaussian, with a given diffusivity, over the stationary diffusivity distribution. Using the same technique as in [61,72] the PDF of all three models at short times yields in the form

$$P(x,t) = \frac{1}{\pi\sqrt{\mathcal{M}(t)_{\rm ST}}}K_0\left(\frac{|x|}{\sqrt{\mathcal{M}(t)_{\rm ST}}}\right), \tag{64}$$

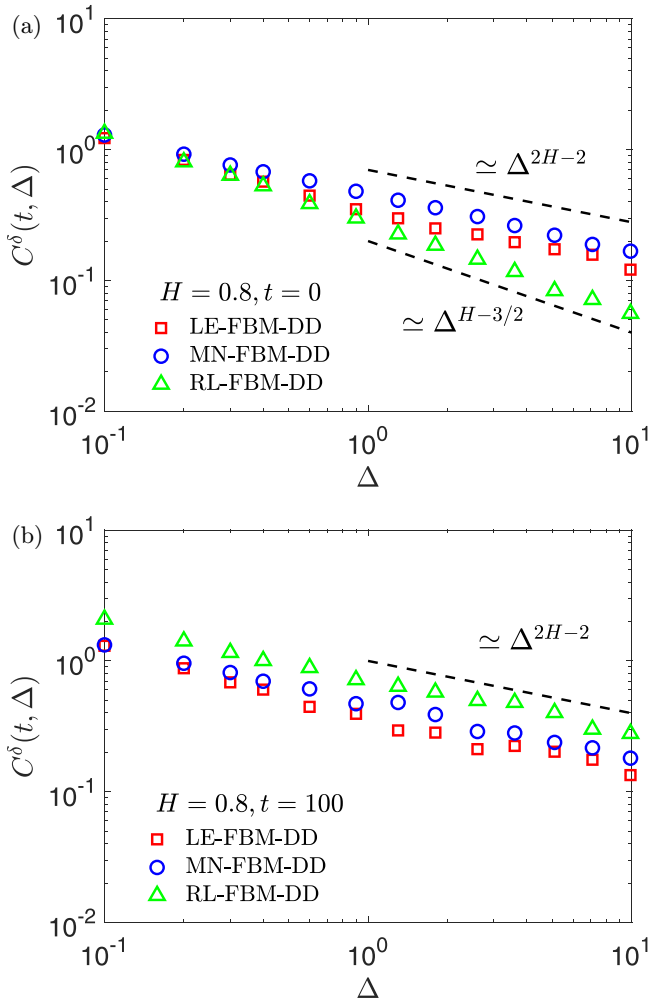

FIG. 3. Simulations (circles, triangles, rectangles) for the ACVF with $H = 0.8$ and starting times (a) $t = 0$ and (b) $t = 100$ for the three DD-generalized FBM models. In panel (a), the ACVF of LE-FBM-DD and MN-FBM-DD decay as $\simeq\Delta^{2H-2}$, while the ACVF of the RL-FBM-DD model has the scaling $\simeq\Delta^{H-3/2}$ when $t = 0$. In panel (b), the ACVF of all models has the same scaling $\simeq\Delta^{2H-2}$ at long times, $t = 100$.

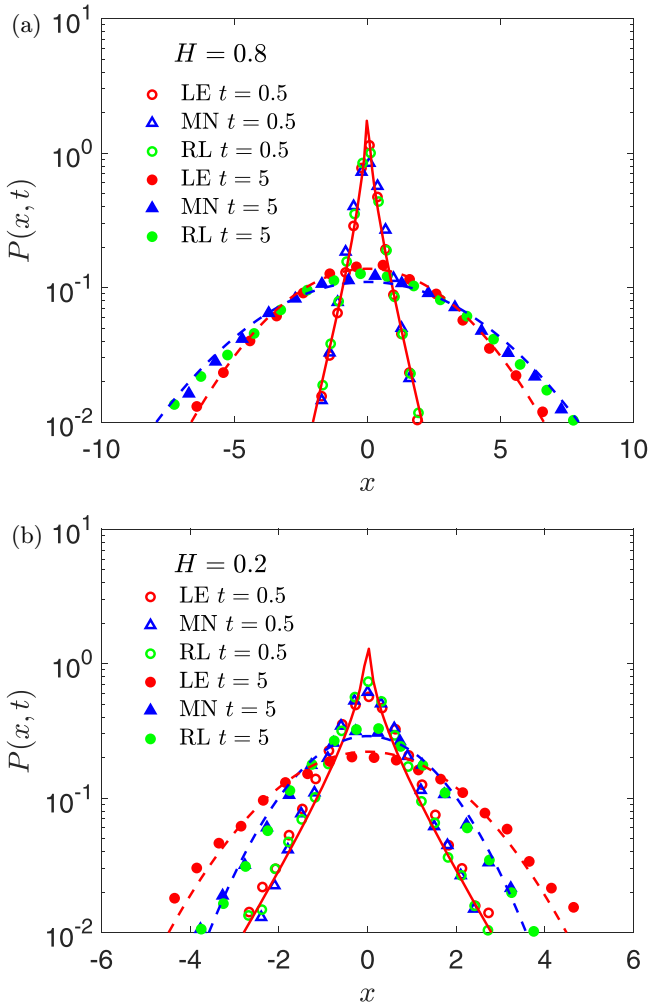

FIG. 4. Simulations (circles, triangles, and rectangles) for the PDF of three DD-generalized FBM models with (a) $H = 0.8$ and (b) $H = 0.2$. The theoretical results (65) and (66) for the PDF at short and long times, respectively, are represented by the colored solid and dashed curves.

where $\mathcal{M}(t)_{\rm ST}$ is the MSD of the three DD-generalized FBM models (39), (45), and (46) at short times. Moreover, K_0 denotes the modified Bessel function of the second kind. In particular, for the relevant large displacements ensuring $z = |x|/\sqrt{\mathcal{M}(t)_{\rm ST}} \gg 1$, the Bessel function has the expansion $K_0 \sim \sqrt{\pi/(2z)}e^{-z}$, and thus the PDF can be approximated as

$$P(x,t) \sim \frac{1}{\sqrt{2\pi|x|\mathcal{M}(t)_{\rm ST}^{1/2}}} \exp\left(-\frac{|x|}{\sqrt{\mathcal{M}(t)_{\rm ST}}}\right). \quad (65)$$

At long times, the Gaussian limit is recovered due to the central limit theorem for all three models,

$$P(x,t) \sim \frac{1}{\sqrt{2\pi\mathcal{M}(t)_{\rm LT}}} \exp\left(-\frac{x^2}{2\mathcal{M}(t)_{\rm LT}}\right), \quad (66)$$

where $\mathcal{M}(t)_{\rm LT}$ is the MSD of the three DD-generalized FBM models (39), (45), and (46).

The comparison of simulations and theoretical results for the PDFs are shown in Fig. 4. We note that when evaluating the short-time exponential PDF (65) for $H = 0.2$ [solid curve in Fig. 4(b)], the numerical result at $t = 0.5$ appears to diverge from the theoretical prediction, in particular around $x = 0$. This discrepancy is not observed for $H = 0.8$, as illustrated in Fig. 4(a). The reason for this lies in the validity range of the short-time exponential tail approximation (65), i.e.,

$$|x| \gg \sqrt{2\langle D\rangle}t^H, \quad (67)$$

which holds for times $t \ll 1$. This approximation at short times is based on the asymptotic form of the modified Bessel function of the second kind $K_0(z)$ for large $z = |x|/\sqrt{\mathcal{M}(t)_{\rm ST}} = |x|/\sqrt{2\langle D\rangle t^{2H}} \gg 1$ in Eq. (64). Consequently, for a fixed short time t, the condition (67) for the validity of the approximation is better satisfied for $H > 1/2$ than for $H < 1/2$, making deviations from simulations negligible in the former case. However, when $t \gg 1$, there is no

TABLE I. Comparison of the statistical properties of the three FBM-generalized DD models: LE-FBM-DD, MN-FBM-DD, and RL-FBM-DD.

	LE-FBM-DD	MN-FBM-DD	RL-FBM-DD
$\langle x^2(t)\rangle$	Short time: $\sim 2\langle D\rangle t^{2H}$, Eq. (40) Long time ($H > 1/2$): $\sim 2K_{\rm eff} t^{2H}$, Eq.(41) Long time ($H < 1/2$): $\sim 2D_{\rm eff} t$, Eq. (42)	$2\langle D\rangle t^{2H}$, Eq. (45)	$2\langle D\rangle t^{2H}$, Eq. (46)
$\langle x_\Delta^2(t)\rangle$	Stationary: Short lag time: $\sim 2\langle D\rangle \Delta^{2H}$, Eq. (48) Long lag time ($H > 1/2$): $\sim 2K_{\rm eff}\Delta^{2H}$, Eq. (49) Long lag time ($H < 1/2$): $\sim 2D_{\rm eff}\Delta$, Eq. (49)	Stationary: $2\langle D\rangle \Delta^{2H}$, Eq. (52)	Nonstationary: $4H\langle D\rangle[I_H(\frac{t}{\Delta}) + \frac{1}{2H}]\Delta^{2H}$, Eq. (53) Short time: $\sim 2\langle D\rangle\Delta^{2H}$, Eq. (54) Long time: $\sim \frac{2\langle D\rangle\Gamma(H+1/2)^2}{\Gamma(2H)\sin(\pi H)}\Delta^{2H}$, Eq. (55)
$C^\delta(t,\Delta)$	Stationary: $2K(\Delta)\langle \xi_H^2\rangle_\Delta$, Eq. (56)	Stationary: $2\langle D\rangle\langle \xi_H^2\rangle_\Delta$, Eq. (60)	Nonstationary: Eq. (61) $t = 0$: $\sim \frac{4\langle D\rangle H(2H-1)\delta^{H-1/2}}{2H+1}\Delta^{H-3/2}$, Eq. (62) $t \to \infty$: $\sim \frac{2\langle D\rangle H(2H-1)\Gamma(H+1/2)^2}{\Gamma(2H)\sin(\pi H)}\Delta^{2H-2}$, Eq. (63)

obvious deviation between the long-time asymptotic PDF (66) and the simulations when varying H.

VI. DISCUSSION AND CONCLUSIONS

We examined the statistical properties of the DD-generalizations based on the three representations of FBM: LE-FBM, MN-FBM, and RL-FBM. The main results are summarized in Table I. With constant coefficients, both LE-FBM and MN-FBM are equivalent, with stationary increments, whereas RL-FBM has nonstationary increments. However, when introducing the DD dynamics, the affected dynamics of the DD-generalized FBM processes differ significantly. The MN-FBM-DD and RL-FBM-DD models share the same MSD, MSI, and ACVF with their corresponding FBM models, scaled by an effective diffusivity equal to the mean value. In contrast, the LE-FBM-DD model is influenced more severely by the diffusivity correlations, leading to *a priori* unexpected crossovers in the scaling behaviors of the MSD and MSI. Additionally, both MN-FBM-DD and LE-FBM-DD exhibit stationary properties, whereas RL-FBM-DD does not. All DD-generalized FBM models demonstrate a crossover in the PDF, crossing over from a short-time non-Gaussian to a long-time Gaussian shape.

The crossover behavior in the scaling of both MSD and MSI observed for the LE-FBM-DD model can be generally predicted by the correlation of the DD dynamics following the squared OU process,

$$K(\Delta = |t_1 - t_2|) = \langle \sqrt{D(t_1)}\sqrt{D(t_2)}\rangle \sim c_1 + c_2 e^{-\Delta/\tau}, \quad (68)$$

where $c_1, c_2 > 0$. A similar behavior was also observed when the random diffusivity follows a Markovian switching behavior ("two-state model") between the two values D_1, D_2 with rate k_1 and k_2 [72]. This model is also in equilibrium and has correlations with $c_1, c_2 > 0$. Moreover, for other protocols of the diffusivity, no crossover behavior will be observed when $c_1 > 0$ and $c_2 = 0$, e.g., the diffusivity is considered to be a random variable, while the crossover behavior from anomalous to normal diffusion occurs for all H when $c_1 = 0$ and $c_2 > 0$, e.g., in the Tyagi-Cherayil model [64] defined by the Langevin dynamics $dx/dt = \sqrt{2Y(t)}\xi_H(t)$ [72].

Over the recent years, extensive data from modern single particle tracking and supercomputing studies in complex systems, e.g., bio-relevant systems, demonstrated that the observed dynamics is often more complicated and can no longer be described by individual (anomalous) diffusion processes. Classical statistical observables [95–98], Bayesian statistics [99–101], or deep learning-based analyses [102–109] provide quite reliable means to decipher the (anomalous) diffusive process(es) underlying the data. To provide an ever better body of models for such analyses, the DD-generalized FBM models discussed here should be added to these algorithms.

We anticipate that our results will prompt research on a deeper understanding of how heterogeneity influences diffusion transport phenomena. Several intriguing issues warrant further exploration. For instance, FBM with DD considered to be non-Markovian state-switching has been recently studied in [110], and the system remains non-Gaussian across all time scales, underscoring the role of heavy-tailed distributions in shaping the statistical properties of diffusion processes. Similar persistent non-Gaussian behavior was also found for particles with DD in a confined harmonic potential [111]. Recent single-particle-tracking experiments revealed that intracellular transport of endo- and exogenous tracers of various sizes is often not only anomalous, but also heterogeneous in time and space. This implies that a single diffusion exponent of standard anomalous-diffusion models is insufficient to describe the underlying physical phenomena. The DD-generalized FBM model, for which the anomalous diffusion exponent depends on time or space, deserves to be investigated. Additional aspects, such as the first passage dynamics [112,113] and resetting dynamics [114,115] should also be explored. Finally, another intriguing direction of the research could be to study universal singularities of the three models with random diffusion exponents along the concepts developed in [116,117].

ACKNOWLEDGMENTS

R.M. acknowledges the financial support from the German Science Foundation (DFG, Grant ME 1535/13-1

and ME 1535/22-1) and NSF-BMBF CRCNS (Grant No. 2112862/STAXS). A.V.C. acknowledges BMBF Project PLASMA-SPIN Energy (Grant No. 01DK2406).

DATA AVAILABILITY

The code used to generate the simulation results is available at [118]. Data that are not openly available but are available upon reasonable request from the authors.

[1] R. Brown, A brief account of microscopical observations made in the months of June, July and August 1827, on the particles contained in the pollen of plants; and on the general existence of active molecules in organic and inorganic bodies, Philos. Mag. **4**, 161 (1828).

[2] A. Einstein, Über die von der molekularkinetischen Theorie der Wärme geforderte Bewegung von in ruhenden Flüssigkeiten suspendierten Teilchen, Ann. Phys. **322**, 549 (1905).

[3] W. Sutherland, A dynamical theory of diffusion for nonelectrolytes and the molecular mass of albumin, Philos. Mag. **9**, 781 (1905).

[4] M. von Smoluchowski, Zur kinetischen Theorie der Brownschen Molekularbewegung und der Suspensionen, Ann. Phys. **326**, 756 (1906).

[5] P. Langevin, Sur la théorie du mouvement brownien, C. R. Acad. Sci. (Paris) **146**, 530 (1908).

[6] J. Perrin, *Les atomes* (Félix Alcan, Paris, 1913); English version: J. Perrin and D. L. Hammick (translator), *Atoms* (Kessinger Publishing, Whitefish, MT).

[7] R. Metzler, J.-H. Jeon, A. Cherstvy, and E. Barkai, Anomalous diffusion models and their properties: non-stationarity, non-ergodicity, and ageing at the centenary of single particle tracking, Phys. Chem. Chem. Phys. **16**, 24128 (2014).

[8] M. Weiss, M. Elsner, F. Kartberg, and T. Nilsson, Anomalous subdiffusion is a measure for cytoplasmic crowding in living cells, Biophys. J. **87**, 3518 (2004).

[9] I. Golding and E. C. Cox, Physical nature of bacterial cytoplasm, Phys. Rev. Lett. **96**, 098102 (2006).

[10] J.-H. Jeon, V. Tejedor, S. Burov, E. Barkai, C. Selhuber-Unkel, K. Berg-Sørensen, L. Oddershede, and R. Metzler, In vivo anomalous diffusion and weak ergodicity breaking of lipid granules, Phys. Rev. Lett. **106**, 048103 (2011).

[11] R. Großmann, L. S. Bort, T. Moldenhawer, M. Stange, S. S. Panah, R. Metzler, and C. Beta, Non-Gaussian displacements in active transport on a carpet of motile cells, Phys. Rev. Lett. **132**, 088301 (2024).

[12] J.-H. Jeon, M. Javanainen, H. Martinez-Seara, R. Metzler, and I. Vattulainen, Protein crowding in lipid bilayers gives rise to non-Gaussian anomalous lateral diffusion of phospholipids and proteins, Phys. Rev. X **6**, 021006 (2016).

[13] A. Godec, M. Bauer, and R. Metzler, Collective dynamics effect transient subdiffusion of inert tracers in flexible gel networks, New J. Phys. **16**, 092002 (2014).

[14] T. Akimoto, E. Yamamoto, K. Yasuoka, Y. Hirano, and M. Yasui, Non-Gaussian fluctuations resulting from power-law trapping in a lipid bilayer, Phys. Rev. Lett. **107**, 178103 (2011).

[15] F. Michael and M. D. Johnson, Financial market dynamics, Physica A **320**, 525 (2003).

[16] R. N. Mantegna and H. E. Stanley, *An Introduction to Econophysics: Correlations and Complexity in Finance* (Cambridge University Press, Cambridge, 2000).

[17] N. E. Humphries *et al.*, Environmental context explains Lévy and Brownian movement patterns of marine predators, Nature (London) **465**, 1066 (2010).

[18] P. G. Meyer, A. G. Cherstvy, H. Seckler, R. Hering, N. Blaum, F. Jeltsch, and R. Metzler, Directedness, correlations, and daily cycles in springbok motion: from data via stochastic models to movement prediction, Phys. Rev. Res. **5**, 043129 (2023).

[19] O. Vilk, Y. Orchan, M. Charter, N. Ganot, S. Toledo, R. Nathan, and M. Assaf, Ergodicity breaking in area-restricted search of Avian predators, Phys. Rev. X **12**, 031005 (2022).

[20] O. Vilk *et al.*, Unravelling the origins of anomalous diffusion: From molecules to migrating storks, Phys. Rev. Res. **4**, 033055 (2022).

[21] A. Lazarian and H. Yan, Superdiffusion of cosmic rays: implications for cosmic ray acceleration, Astrophys. J. **784**, 38 (2014).

[22] B. Berkowitz, A. Cortis, M. Dentz, and H. Scher, Modeling non-Fickian transport in geological formations as a continuous time random walk, Rev. Geophys. **44**, 2005RG000178 (2006).

[23] A. Rajyaguru, R. Metzler, I. Dror, D. Grolimund, and B. Berkowitz, Diffusion in porous rock is anomalous, Environ. Sci. Technol. **58**, 8946 (2024).

[24] D. Wei, A. Rubio-Abadal, B. Ye, F. Machado, J. Kemp, K. Srakaew, S. Hollerith, J. Rui, S. Gopalakrishnan, N. Y. Yao, I. Bloch, and J. Zeiher, Quantum gas microscopy of Kardar-Parisi-Zhang superdiffusion, Science **376**, 716 (2022).

[25] J.-P. Bouchaud and A. Georges, Anomalous diffusion in disordered media: Statistical mechanisms, models and physical applications, Phys. Rep. **195**, 127 (1990).

[26] I. M. Sokolov, Models of anomalous diffusion in crowded environments, Soft Matter **8**, 9043 (2012).

[27] E. Barkai, Y. Garini, and R. Metzler, Strange kinetics of single molecules in living cells, Phys. Today **65**(8), 29 (2012).

[28] Y. Mishura, *Stochastic Calculus for Fractional Brownian Motion and Related Processes* (Springer, Berlin, 2008).

[29] M. M. Meerschaert and A. Sikorskii, *Stochastic Models for Fractional Calculus*, Vol. 43 (Walter de Gruyter, Berlin, 2019).

[30] E. W. Montroll and G. H. Weiss, Random walks on lattices. II, J. Math. Phys. **6**, 167 (1965).

[31] J. Klafter, A. Blumen, and M. F. Shlesinger, Stochastic pathway to anomalous diffusion, Phys. Rev. A **35**, 3081 (1987).

[32] B. D. Hughes, *Random Walks and Random Environments*, Vol. 1: Random walks (Oxford University Press, Oxford, UK, 1995).

[33] R. Metzler and J. Klafter, The random walk's guide to anomalous diffusion: a fractional dynamics approach, Phys. Rep. **339**, 1 (2000).

[34] J. M. Berger and B. Mandelbrot, A new model for error clustering in telephone circuits, IBM J. Res. Develop. **7**, 224 (1963).

[35] H. Scher and E. W. Montroll, Anomaous transit-time dispersion in amorphous solids, Phys. Rev. B **12**, 2455 (1975).
[36] A. N. Kolmogorov, Wienersche Spiralen und einige andere interessante Kurven im Hilbertschen Raum, C. R. (Doklady) Acad. Sci. URSS (N. S.) **26**, 115 (1940).
[37] B. B. Mandelbrot and J. W. van Ness, Fractional Brownian motions, fractional noises and applications, SIAM Rev. **10**, 422 (1968).
[38] G. Guigas, V. Kalla, and M. Weiss, Probing the nanoscale viscoelasticity of intracellular fluids in living cells, Biophys. J. **93**, 316 (2007).
[39] S. C. Weber, A. J. Spakowitz, and J. A. Theriot, Bacterial chromosomal loci move subdiffusively through a viscoelastic cytoplasm, Phys. Rev. Lett. **104**, 238102 (2010).
[40] S. Janušonis, N. Detering, R. Metzler, and T. Vojta, Serotonergic axons as fractional brownian motion paths: insights into the self-organization of regional densities, Front. Comput. Neurosci. **14**, 56 (2020).
[41] S. Janušonis, J. H. Haiman, R. Metzler, and T. Vojta, Predicting the distribution of serotonergic axons: a supercomputing simulation of reflected fractional Brownian motion in a 3D-mouse brain model, Front. Comput. Neurosci. **17**, 1189853 (2023).
[42] J. Gatheral, T. Jaisson, and M. Rosenbaum, Volatility is rough, Quant. Financ. **18**, 933 (2018).
[43] T. Guggenberger, G. Pagnini, T. Vojta, and R. Metzler, Fractional Brownian motion in a finite interval: correlation effects depletion or accretion zones of particles near boundaries, New J. Phys. **21**, 022002 (2019).
[44] A. H. O. Wada and T. Vojta, Fractional Brownian motion with a reflecting wall, Phys. Rev. E **97**, 020102(R) (2018).
[45] T. Vojta, S. Halladay, S. Skinner, S. Janušonis, T. Guggenberger, and R. Metzler, Reflected fractional Brownian motion in one and higher dimensions, Phys. Rev. E **102**, 032108 (2020).
[46] T. Guggenberger, A. Chechkin, and R. Metzler, Fractional Brownian motion in superharmonic potentials and non-Boltzmann stationary distributions, J. Phys. A **54**, 29LT01 (2021).
[47] T. Guggenberger, A. V. Chechkin, and R. Metzler, Absence of confinement and non-Boltzmann stationary states of fractional Brownian motion in shallow external potentials, New J. Phys. **24**, 073006 (2022).
[48] A. Pacheco-Pozo and D. Krapf, Fractional Brownian motion with fluctuating diffusivities, Phys. Rev. E **110**, 014105 (2024).
[49] W. Wang, M. Balcerek, K. Burnecki, A. Chechkin, S. Janušonis, J. Ślęzak, T. Vojta, A. Wyłomańska, and R. Metzler, Memory-multi-fractional Brownian motion with continuous correlations, Phys. Rev. Res. **5**, L032025 (2023).
[50] M. Balcerek, A. Wyłomańska, K. Burnecki, R. Metzler, and D. Krapf, Modelling intermittent anomalous diffusion with switching fractional Brownian motion, New J. Phys. **25**, 103031 (2023).
[51] J. Ślęzak and R. Metzler, Minimal model of diffusion with time changing Hurst exponent, J. Phys. A **56**, 35LT01 (2023).
[52] T. A. Waigh and N. Korabel, Heterogeneous anomalous transport in cellular and molecular biology, Rep. Prog. Phys. **86**, 126601 (2023).
[53] B. Wang, J. Kuo, S. C. Bae, and S. Granick, When Brownian diffusion is not Gaussian, Nat. Mater. **11**, 481 (2012).
[54] B. Wang, S. M. Anthony, S. C. Bae, and S. Granick, Anomalous yet Brownian, Proc. Natl. Acad. Sci. USA **106**, 15160 (2009).
[55] J. M. Miotto, S. Pigolotti, A. V. Chechkin, and S. Roldán-Vargas, Length scales in Brownian yet non-Gaussian dynamics, Phys. Rev. X **11**, 031002 (2021).
[56] A. Alexandre, M. Lavaud, N. Fares, E. Millan, Y. Louyer, T. Salez, Y. Amarouchene, T. Guérin, and D. S. Dean, Non-Gaussian diffusion near surfaces, Phys. Rev. Lett. **130**, 077101 (2023).
[57] F. Rusciano, R. Pastore, and F. Greco, Fickian Non-Gaussian diffusion in glass-forming liquids, Phys. Rev. Lett. **128**, 168001 (2022).
[58] I. Chakraborty and Y. Roichman, Disorder-induced Fickian yet non-Gaussian diffusion in heterogeneous media, Phys. Rev. Res. **2**, 022020(R) (2020).
[59] S. Nampoothiri, E. Orlandini, F. Seno, and F. Baldovin, Brownian non-Gaussian polymer diffusion and queuing theory in the mean-field limit, New J. Phys. **24**, 023003 (2022).
[60] M. V. Chubynsky and G. W. Slater, Diffusing diffusivity: A model for anomalous, yet Brownian, diffusion, Phys. Rev. Lett. **113**, 098302 (2014).
[61] A. V. Chechkin, F. Seno, R. Metzler, and I. M. Sokolov, Brownian yet non-Gaussian diffusion: From superstatistics to subordination of diffusing diffusivities, Phys. Rev. X **7**, 021002 (2017).
[62] V. Sposini, A. V. Chechkin, F. Seno, G. Pagnini, and R. Metzler, Random diffusivity from stochastic equations: comparison of two models for Brownian yet non-Gaussian diffusion, New J. Phys. **20**, 043044 (2018).
[63] V. Sposini, D. S. Grebenkov, R. Metzler, G. Oshanin, and F. Seno, Universal spectral features of different classes of random diffusivity processes, New J. Phys. **22**, 063056 (2020).
[64] N. Tyagi and B. J. Cherayil, Non-Gaussian Brownian diffusion in dynamically disordered thermal environments, J. Phys. Chem. B **121**, 7204 (2017).
[65] R. Jain and K. L. Sebastian, Lévy flight with absorption: A model for diffusing diffusivity with long tails, Phys. Rev. E **95**, 032135 (2017).
[66] R. Jain and K. L. Sebastian, Diffusion in a crowded, rearranging environment, J. Phys. Chem. B **120**, 3988 (2016).
[67] T. J. Lampo, S. Stylianidou, M. P. Backlund, P. A. Wiggins, and A. J. Spakowitz, Cytoplasmic RNA-protein particles exhibit non-Gaussian subdiffusive behavior, Biophys. J. **112**, 532 (2017).
[68] W. He, H. Song, Y. Su, L. Geng, B. J. Ackerson, H. B. Peng, and P. Tong, Dynamic heterogeneity and non-Gaussian statistics for acetylcholine receptors on live cell membrane, Nat. Commun. **7**, 11701 (2016).
[69] S. Thapa, N. Lukat, C. Selhuber-Unkel, A. G. Cherstvy, and R. Metzler, Transient superdiffusion of polydisperse vacuoles in highly motile amoeboid cells, J. Chem. Phys. **150**, 144901 (2019).
[70] A. G. Cherstvy, O. Nagel, C. Beta, and R. Metzler, Non-Gaussianity, population heterogeneity, and transient superdiffusion in the spreading dynamics of amoeboid cells, Phys. Chem. Chem. Phys. **20**, 23034 (2018).

[71] A. Díez Fernández, P. Charchar, A. G. Cherstvy, R. Metzler, and M. W. Finnis, The diffusion of doxorubicin drug molecules in silica nanochannels is non-Gaussian and intermittent, Phys. Chem. Chem. Phys. **22**, 27955 (2020).

[72] W. Wang, F. Seno, I. M. Sokolov, A. V. Chechkin, and R. Metzler, Unexpected crossovers in correlated random-diffusivity processes, New J. Phys. **22**, 083041 (2020).

[73] W. Wang, A. G. Cherstvy, A. V. Chechkin, S. Thapa, F. Seno, X. Liu, and R. Metzler, Fractional Brownian motion with random diffusivity: emerging residual nonergodicity below the correlation time, J. Phys. A: Math. Theor. **53**, 474001 (2020).

[74] L. Luo and M. Yi, Non-Gaussian diffusion in static disordered media, Phys. Rev. E **97**, 042122 (2018).

[75] L. Luo and M. Yi, Quenched trap model on the extreme landscape: The rise of subdiffusion and non-Gaussian diffusion, Phys. Rev. E **100**, 042136 (2019).

[76] S. Park, X. Durang, R. Metzler, and J.-H. Jeon, Fickian yet non-Gaussian diffusion in an annealed heterogeneous environment, arXiv:2503.15366.

[77] Q. Wei, W. Wang, Y. Tang, R. Metzler, and A. Chechkin, Fractional Langevin equation far from equilibrium: Riemann-Liouville fractional Brownian motion, spurious nonergodicity, and aging, Phys. Rev. E **111**, 014128 (2025).

[78] A. N. Kolmogorov, The local structure of turbulence in incompressible viscous fluid for very large Reynolds numbers, Dokl. Akad. Nauk. SSSR **30**, 301 (1941).

[79] A. N. Kolmogorov, Dissipation of energy in locally isotropic turbulence, Dokl. Akad. Nauk. SSSR **32**, 19 (1941).

[80] A. M. Yaglom, and M. S. Pinsker, Random process with stationary increments of order n, Dokl. Akad. Nauk. SSSR **90**, 731 (1953).

[81] A. M. Yaglom, *Correlation Theory of Stationary and Related Random Functions*, Vol. 1, Basic Results, Vol. 2, Supplementary Notes and References (Springer, New York, 1987).

[82] D. Marinucci and P. M. Robinson, Alternative forms of fractional Brownian motion, J. Statist. Plan. Infer. **80**, 111 (1999).

[83] M. Balcerek, K. Burnecki, S. Thapa, A. Wyłomańska, and A. V. Chechkin, Fractional Brownian motion with random Hurst exponent: Accelerating diffusion and persistence transitions, Chaos **32**, 093114 (2022).

[84] D. Molina-Garcia, T. Sandev, H. Safdari, G. Pagnini, A. Chechkin, and R. Metzler, Crossover from anomalous to normal diffusion: truncated power-law noise correlations and applications to dynamics in lipid bilayers, New J. Phys. **20**, 103027 (2018).

[85] P. Lévy, in *Random Functions: General Theory with Special Reference to Laplacian Random Functions* (University of California Press, Berkeley, 1953).

[86] S. C. Lim, Fractional Brownian motion and multifractional Brownian motion of Riemann-Liouville type, J. Phys. A: Math. Theor. **34**, 1301 (2001).

[87] D. T. Gillespie, Exact numerical simulation of the Ornstein-Uhlenbeck process and its integral, Phys. Rev. E **54**, 2084 (1996).

[88] D. T. Gillespie, The mathematics of Brownian motion and Johnson noise, Am. J. Phys. **64**, 225 (1996).

[89] J. R. M. Hosking, Modeling persistence in hydrological time series using fractional differencing, Water Resour. Res. **20**, 1898 (1984).

[90] D. Dieker, Simulation of fractional Brownian motion, Master's thesis, University of Twente, The Netherlands, 2004.

[91] J. F. Coeurjolly, Inférence statistique pour les mouvements browniens fractionnaires et multifractionnaires, Ph.D. thesis, Université Joseph-Fourier-Grenoble I, France, 2000.

[92] A. T. Wood and G. Chan, Simulation of stationary Gaussian processes in $[0, 1]^d$, J. Comput. Graph. Stat. **3**, 409 (1994).

[93] S. Rambaldi and O. Oinazza, An accurate fractional Brownian motion generator, Physica A **208**, 21 (1994).

[94] C. Beck and E. G. D. Cohen, Superstatistics, Physica A **322**, 267 (2003).

[95] M. Weiss, Single-particle tracking data reveal anticorrelated fractional Brownian motion in crowded fluids, Phys. Rev. E **88**, 010101 (2013).

[96] A. V. Weigel, B. Simon, M. M. Tamkun, and D. Krapf, Ergodic and nonergodic processes coexist in the plasma membrane as observed by single-molecule tracking, Proc. Natl. Acad. Sci. **108**, 6438 (2011).

[97] G. Sikora, K. Burnecki, and A. Wyłomańska, Mean-squared-displacement statistical test for fractional Brownian motion, Phys. Rev. E **95**, 032110 (2017).

[98] C. L. Vestergaard, P. C. Blainey, and H. Flyvbjerg, Optimal estimation of diffusion coefficients from single-particle trajectories, Phys. Rev. E **89**, 022726 (2014).

[99] A. Robson, K. Burrage, and M. C. Leake Inferring diffusion in single live cells at the single-molecule level, Phil. Trans. R. Soc. B **368**, 20120029 (2013).

[100] J. Krog, L. H. Jacobsen, F. W. Lund, D. Wüstner, and M. A. Lomholt, Bayesian model selection with fractional Brownian motion, J. Stat. Mech. (2018) 093501.

[101] S. Thapa, M. A. Lomholt, J. Krog, A. G. Cherstvy, and R. Metzler, Bayesian analysis of single-particle tracking data using the nested-sampling algorithm: maximum-likelihood model selection applied to stochastic-diffusivity data, Phys. Chem. Chem. Phys. **20**, 29018 (2018).

[102] G. Muñoz-Gil, M. A. Garcia-March, C. Manzo, J. D. Martín-Guerrero, and M. Lewenstein, Single trajectory characterization via machine learning, New J. Phys. **22**, 013010 (2020).

[103] H. Seckler, J. Szwabiński, and R. Metzler, Machine-learning solutions for the analysis of single-particle diffusion trajectories, J. Phys. Chem. Lett. **14**, 7910 (2023).

[104] C. Manzo, Extreme learning machine for the characterization of anomalous diffusion from single trajectories (AnDi-ELM), J. Phys. A: Math. Theor. **54**, 334002 (2021).

[105] H. Seckler and R. Metzler, Bayesian deep learning for error estimation in the analysis of anomalous diffusion, Nat. Commun. **13**, 6717 (2022).

[106] P. Kowalek, H. Loch-Olszewska, and J. Szwabiński, Classification of diffusion modes in single-particle tracking data: Feature-based versus deep-learning approach, Phys. Rev. E **100**, 032410 (2019).

[107] G. Muñoz-Gil *et al.*, Objective comparison of methods to decode anomalous diffusion, Nat. Commun. **12**, 6253 (2021).

[108] N. Granik, L. E. Weiss, E. Nehme, M. Levin, M. Chein, E. Perlson, Y. Roichman, and Y. Shechtman, Single-particle diffusion characterization by deep learning, Biophys. J. **117**, 185 (2019).

[109] D. Han, N. Korabel, R. Chen, M. Johnston, A. Gavrilova, V. J. Allan, S. Fedotov, and T. A. Waigh, Deciphering anomalous

heterogeneous intracellular transport with neural networks, eLife **9**, e52224 (2020).

[110] M. Balcerek, A. Pacheco-Pozo, A. Wyłomańska, and D. Krapf, Evaluating Gaussianity of heterogeneous fractional Brownian motion, arXiv:2501.10472.

[111] Y. Lanoiselée, A. Stanislavsky, D. Calebiro, and A. Weron, Temperature and friction fluctuations inside a harmonic potential, Phys. Rev. E **106**, 064127 (2022).

[112] V. Sposini, S. Nampoothiri, A. Chechkin, E. Orlandini, F. Seno, and F. Baldovin, Being heterogeneous is disadvantageous: Brownian non-Gaussian searches, Phys. Rev. E **109**, 034120 (2024).

[113] V. Sposini, S. Nampoothiri, A. Chechkin, E. Orlandini, F. Seno, and F. Baldovin, Being heterogeneous is advantageous: extreme Brownian non-Gaussian searches, Phys. Rev. Lett. **132**, 117101 (2024).

[114] M. R. Evans and S. N. Majumdar, Diffusion with stochastic resetting, Phys. Rev. Lett. **106**, 160601 (2011).

[115] A. Pal and S. Reuveni, First passage under restart, Phys. Rev. Lett. **118**, 030603 (2017).

[116] A. L. Stella, A. Chechkin, and G. Teza, Anomalous dynamical scaling determines universal critical singularities, Phys. Rev. Lett. **130**, 207104 (2023).

[117] A. L. Stella, A. Chechkin, and G. Teza, Universal singularities of anomalous diffusion in the Richardson class, Phys. Rev. E **107**, 054118 (2023).

[118] https://github.com/WeiWangNuaa/FBM-DD-model.